Blood First Edition Paper, prepublished online October 13, 2015; DOI 10.1182/blood-2015-06-654194

Glutathione peroxidase 4 prevents necroptosis in mouse erythroid precursors

Özge Canli[1], Yasemin B. Alankuş[2], Sasker Grootjans[3], Naidu Vegi[4], Lothar Hültner[5], Philipp S. Hoppe[6], Timm Schroeder[6], Peter Vandenabeele[3], Georg W. Bornkamm[5] and Florian R. Greten[1#]

[1]Institute for Tumor Biology and Experimental Therapy, Georg-Speyer-Haus, Paul-Ehrlich-Str. 42-44, 60596 Frankfurt am Main, Germany
[2]Institute of Clinical Chemistry, Klinikum rechts der Isar, Technical University Munich, Ismaningerstr. 22, 81675 Munich, Germany
[3]Department for Molecular Biomedical Research, VIB, VIB-Ghent University Technologiepark 927, B-9052 Ghent (Zwijnaarde), Belgium
[4]Institute of Experimental Cancer Research, Comprehensive Cancer Center and University Hospital Ulm, James-Franck-Ring, 89081 Ulm, Germany
[5]Institute of Clinical Molecular Biology and Tumor Genetics, Helmholtz Zentrum München, Marchioninistr. 25, 81377 Munich, Germany
[6]Department of Biosystems Science and Engineering, ETH Zurich, 4058 Basel, Switzerland

[#] Correspondence should be addressed to:

greten@gsh.uni-frankfurt.de

Key Points

- Gpx4 is essential for preventing anemia in mice via inhibiting RIP3 dependent necroptosis in erythroid precursor cells.
- ROS accumulation and lipid peroxidation in erythroid precursor cells trigger receptor-independent activation of necroptosis.

Abstract

Maintaining cellular redox balance is vital for cell survival and tissue homoeostasis since imbalanced production of ROS may lead to oxidative stress and cell death. The anti-oxidant enzyme glutathione peroxidase 4 (Gpx4) is a key regulator of oxidative stress-induced cell death. We show that mice with deletion of *Gpx4* in hematopoietic cells develop anemia and that it is essential for preventing RIP3 dependent necroptosis in erythroid precursor cells. Absence of *Gpx4* leads to functional inactivation of caspase 8 by glutathionylation. This results in necroptosis, which occurs independently of TNFα activation. While genetic ablation of *Rip3* normalizes reticulocyte maturation and prevents anemia, ROS accumulation and lipid peroxidation in *Gpx4* deficient cells remain high. Our results demonstrate that ROS and lipid hydroperoxides function as so far unrecognized unconventional upstream signaling activators of RIP3-dependent necroptosis.

Introduction

Oxidative stress is defined as the imbalance in cellular redox in favor of the oxidants. Whereas at low levels (reactive oxygen species) ROS act as second messengers[1], at high levels they can damage organelles as well as DNA and induce programmed cell death such as apoptosis and necroptosis.[2,3] Increased oxidative stress plays a crucial role in a variety of pathological conditions including cancer, degenerative diseases, and aging.

Due to their physiological function in oxygen transport, oxygen-loaded erythrocytes are under constant oxidative stress. Thus, erythrocytes are equipped with a battery of antioxidant enzymes that support dismutation of superoxide radicals, detoxification of hydrogen and lipid peroxides, and maintain a reducing intracellular milieu (e.g. superoxide dismutase 1 and 2, catalase, glutathione peroxidase 1, peroxiredoxin I and II and glutathione synthesizing enzymes). Mutations in many of these genes in humans[4] or disruption of the genes in mice cause hemolytic anemia.[5-7] Similarly, selenium deficiency leads to anemia in vertebrates[8] yet, the contribution of individual selenoproteins hereto is still unknown. Gpx4 has a very high rank within the so-called selenium hierarchy among mammalian selenoproteins, which is determined based on the expression level of a selenoprotein under selenium deficiency, due to its stable expression even when selenium is rare, thus indicating a strong dependence on this enzyme.[9] Importantly, Gpx4 is the only glutathione peroxidase known to be essential for embryonic development.[10,11] Moreover, Gpx4 controls caspase-independent cell death in neurons[12], photoreceptor cells[13] and T cells.[14]

Ferroptosis is a non-apoptotic form of cell death involving the production of iron-dependent ROS.[15] It was recently described that the oncogenic RAS-selective lethal small molecule erastin triggers ferroptosis via inhibiting cysteine uptake by the cysteine/glutamate antiporter, leading to iron-dependent accumulation of lethal lipid ROS and eventually to ferroptotic cell death, which is morphologically, biochemically,

and genetically distinct from apoptosis, necrosis. Later on, Gpx4 was identified as an essential regulator of ferroptotic cancer cell death.[16] In addition to the cancer cells, *Gpx4* depletion leads to massive cell death through the induction of lipid peroxidation and ferroptotic machinery in renal tubular epithelia[17] as well as in T cells[14].

Apart from apoptosis and ferroptosis several other forms of programmed cell death have been described including poly(ADP)ribose polymerase-1 (PARP-1)- and apoptosis-inducing factor 1 (AIF1)-dependent parthanatos, caspase-1-dependent pyroptosis, as well as receptor-interacting protein 1 (RIP1) -dependent necroptosis.[15,18,19,20,21] Necroptosis can be triggered by ligation of death receptors such as CD95, TNF-receptor 1 and 2 as well as TNF-related apoptosis-inducing ligand receptor 1 and 2 (TRAILR1 and 2).[22] The best-characterized pathway inducing necroptosis involves TNFR1 ligation and depends on the activity of caspase 8, which comprises the molecular switch between apoptosis or necroptosis. In case of caspase 8 inhibition, the necrosome, a multiprotein complex containing RIP1 and RIP3, is formed and activated. This culminates in mitochondrial ROS production as well as generation of lipid peroxides as an essential prerequisite for execution of TNF-dependent necrosis.[22,23] So far, mitochondrial ROS production has only been described as a downstream effector mechanism upon necrosome activation. However, direct evidence that ROS could lead to activation of RIP1/RIP3 even as part of a positive feedback loop is lacking. Several important physiological roles of necroptosis were demonstrated by recent studies showing that caspase-8 or Fas-associated protein with death domain (FADD) deficiency cause embryonic lethality and trigger inflammation *in vivo* by sensitizing cells to RIP3 mediated necroptosis.[24-28] Both caspase 8 and FADD knockout mice strains die at the same embryonic stage with a similar phenotype. Cell death observed in the absence of caspase 8 is inhibited upon the additional deletion of *Rip3*, suggesting that caspase 8 inhibits RIP3-mediated necroptosis.[24,25,29]

Although Gpx4 has been identified as an important enzyme for the homeostasis of many cell types, no studies have so far linked Gpx4 to the red blood system. Here we addressed the function of Gpx4 in the erythroid lineage and provide evidence that Gpx4 is essential for erythrocyte homeostasis and for prevention of RIP3 dependent necroptosis independently of death receptor engagement.

Methods

Mice

Gpx4$^{F/F}$ mice were crossed to *Mx1-Cre* or *Rosa26-CreER*^{T2} mice and kept on a mixed genetic background. Rip3$^{-/-}$ mice[30] were crossed to *Mx1-Cre-Gpx4*$^{F/F}$ mice. Deletion of *Gpx4* was induced by a single i.p. injection of 250µg poly I:C (Sigma) dissolved in water. Vitamin E deficient diet was purchased from Ssniff (E15791-147). In adoptive transfer experiments recipient mice were lethally irradiated (9 Gy) and injected with $1x10^6$ donor bone marrow cells into the tail vein. For complete blood counts and flow cytometry analysis, blood was collected from the facial or tail vein in K_2-EDTA collection tubes (Sarstedt) and measurements were performed via Sysmex-XT-2000i. For biotin labeling experiments mice were injected daily for 3 days with biotin-nhs (1mg/day i.v.; Calbiochem, 203118) starting on the day of poly I:C administration. 10µL of blood was used for flow cytometry analysis. α-CD95L neutralizing antibody (50µg; BD Pharmingen, 555291), Olaparib (5mg/kg; Selleckchem) were injected i.p. every two days starting two weeks after poly I:C administration. All animal procedures were performed in accordance with institutional guidelines.

In vitro differentiation of erythroid cells

Mouse erythroid cultures were prepared as described before.[31] Lineage negative bone marrow cells were prepared using biotin labeled lineage cell cocktail (Miltenyi Biotech, 130-092-613) and streptavidin-microbeads (Miltenyi Biotech, 130-048-101)

according to the manufacturer's instructions. Purified cells were seeded in fibronectin-coated plates (Corning) in IMDM (Gibco, 12440053) containing 15% FBS, penicillin/streptomycin (Gibco), 200µg/ml holotransferrin (Sigma, T0665), 10µg/mL recombinant human insulin (Sigma, I9278) and 2 units/mL EPO (R&D, 287-TC-500). One day later the medium is changed to IMDM with 15% FBS, penicillin/streptomycin supplemented either with 1µM 4-OHT (Sigma) to induce the deletion of *Gpx4* or 70% ethanol as control. For the inhibitor experiments all inhibitors were added to the medium together with the 4-OHT. Human recombinant TNFα (R&D systems) was used at 100ng/mL, TAK1 inhibitor 5Z-7-Oxozeaenol (TAKi) (Sigma) at 1µM, caspase inhibitor 1 (zVAD) (Calbiochem) at 50µM, TNF antagonist etanercept at 1µM, DTT 25µM (Sigma), necrostatin-1 (nec-1) at 25µM (Calbiochem), ferrostatin 1 (Fer-1) at 1µM (Calbiochem), liproxstatin-1 (Lip-1) at 1µM (Selleck Chemicals), desferoxamine (DFO) at 1mM (Sigma), erastin at 10µM (Sigma), Ras synthetic lethality molecule 3 (RSL-3) at 5µM (Interbioscreen). Cell viability was determined via tryphan blue exclusion count.

Flow cytometry and cell separation

For flow cytometric analysis cells were stained using fluorophore conjugated antibodies α-TER119 (eBiosciences) and α-CD71 (eBiosciences) (0.1-0.2µg/10^6 cells) in FACS buffer (2% FCS/2mM EDTA/PBS). 10^6 cells were labeled for 30 min at 37°C with redox sensitive fluorescent probe CM-H_2DCFDA (Invitrogen) (1µM) to measure the cellular ROS and with BODIPY 581/591 C11 (2µM) to measure cellular lipid peroxidation prior to surface marker stainings. Annexin V staining was performed according to the manufacturer' s instructions (BD Pharmingen). To determine splenocyte proliferation mice were injected with BrdU (100mg/kg, i.p.) 4 hours prior to sacrifice and splenocytes were subjected to BrdU assay kit (BD Pharmingen). Cell separations were done using magnetic beads according to manufacturer's instructions (Miltenyi Biotec).

Immunohistochemical analysis

Standard immunohistochemical procedures were performed using following antibodies: α-BrdU (AbD Serotec, MCA2060) and α-phospho-Histone H2A.X (Cell Signaling, 2577). TUNEL assay was performed with ApoAlert DNA Fragmentation Assay Kit (Clontech). Briefly, tissues were treated with proteinase K and incubated with TdT enzyme mix, mounted in DAPI containing medium and imaging was performed 2 hours later. Image acquisition was performed using Zeiss Axio Imager M2 with x20/0.5 EC Plan Neofluar or x40/0.95 korr. Apochromat objective and AxioVision sofware.

Protein analysis

Proteins lysates were prepared using lysis buffer ((50 mM Tris (pH 7.5), 250 mM NaCl, 30 mM EDTA, 30 mM EGTA, 25 mM sodium pyrophosphate, 1% triton-X 100, 0,5% NP40, 10% glycerol and protease and phosphatase inhibitors (Roche)). Following antibodies were used for immunoblot analysis: α-RIP1 (BD Biosciences, 610459), α-RIP3 (Abcam, 62344), α-β-actin (Sigma-Aldrich) and α-Gpx4 (Abcam, ab125066), α-FADD (Santa Cruz, M-19, sc-6036), α-caspase 8 (Abnova, MAB3429). Immunoprecipitation experiments were performed with the standard procedures using α-caspase 8 (rabbit polyclonal), with 30 minutes of antibody binding to the Protein A sepharose beads (GE Healthcare) followed by over night incubation with protein lysates.

For glutathionylation analysis cells were labeled with BioGEE (Invitrogen) for 30 minutes at 37°C. The cells were lysed in BioGEE lysis buffer containing 50mM Tris (pH 7.5), 250mM NaCl, 30mM EDTA, 30mM EGTA, 25mM sodiumpyrophosphate, 1% triton-X 100, 0,5% NP40, 10% glycerol. Biotinylated proteins were precipitated from cell lysates with streptavidin agarose beads (Thermo Scientific) for 20 minutes and were eluted with BioGEE lysis buffer containing 10mM DTT. Samples were boiled 5 minutes at 95°C in Laemmli buffer and subjected to immunoblot analysis.

GSH measurements were done using Glutathione Assay Kit II (Calbiochem) according to the manufacturer's instructions with or without 2-vinylpyridine for the detection of GSSG and total GSH, respectively. Absorbance at 405 nm was detected and the concentrations are calculated based on the corresponding standards. Erythropoietin (R&D, Mep00), IL-6 (R&D, DY406), anti-dsDNA (Alpha Diagnostics) ELISA were performed according to the manufacturer's instructions using 50µL serum.

Results

Loss of Gpx4 in hematopoietic cells induces compensated anemia

To functionally examine the consequences of *Gpx4* deficiency in the erythroid lineage regarding uncontrolled ROS accumulation and lipid peroxidation and their possible effects on cell death, we crossed floxed *Gpx4* mice (*Gpx4*$^{F/F}$) to *Mx1-cre* transgenic mice[32] to generate *Mx1-cre/Gpx4*$^{F/F}$ (hereafter referred to as *Gpx4*$^{\Delta}$). Deletion of *Gpx4* in hematopoietic cells was induced by a single intraperitoneal (i.p.) poly-I:C injection. Absence of Gpx4 in CD71^{+}/Ter119^{+} bone marrow erythroblasts as well as in peripheral mature CD71^{-}/Ter119^{+} erythrocytes was confirmed by immunoblot analysis (Figure 1A). Loss of *Gpx4* in hematopoietic cells led to a moderate yet significant decrease in red blood cell counts, hemoglobin levels and hematocrit four weeks after poly-I:C administration (Figure 1B-D). In contrast, reticulocyte counts increased more than two-fold indicating a compensatory increase of erythropoiesis (Figure 1E). In parallel, serum erythropoietin (EPO) levels were more than five fold elevated (Figure 1F). Moreover, increased spleen weight (Figure 1G) and elevated number of proliferative CD71^{+}/Ter119^{+} erythroblasts in the spleen (Figure 1H-J), supported the notion that anemia in *Gpx4*$^{\Delta}$ mice was highly compensated by extramedullary erythropoiesis. The percentage of CD71^{+} cells is increased dramatically in the spleen but also to a lesser extent in the bone marrow (Supplementary Figure 1). Notably, serum IL-6 and dsDNA antibody levels were

unaltered ruling out systemic inflammation or autoimmunity (Supplementary Figure 2). The mice were monitored for six months after the induction of the deletion.

To determine whether increased lipid peroxidation and ROS accumulation in peripheral erythrocytes (Figure 2A, B) triggered their premature death, we determined the half-life of biotin labeled erythrocytes (Ter119^{+}). While turnover of peripheral Gpx4$^{\Delta}$ mature erythrocytes remained unaltered compared to littermate controls (Figure 2C), the number of reticulocytes steadily increased within 4 weeks (Figure 2D). However, this was paralleled by massive cell death in spleen determined by TUNEL and flow cytometry confirmed increased number of PI^{+}CD71^{+} *Gpx4*$^{\Delta}$ cells in spleen and bone marrow (Figure 2E-H). The consequences of increased erythroid precursor death became even more apparent in *in vitro* erythroid colony formation assay as formation of red colonies was nearly completely abolished in *Gpx4*$^{\Delta}$ bone marrow. However, this could be significantly improved in the presence of α-tocopherol (α-Toc), the most prominent member of the vitamin E family (Figure 2I), recapitulating the phenotype of *Gpx4* deficiency in fibroblasts, neurons, kidney tubule cells and endothelial cells.[12,17,33]

Vitamin E is essential for the compensatory increase in reticulocyte numbers in the absence of Gpx4

Recently it was shown that high vitamin E content typically present in regular animal chow (55-135mg/kg) can partially compensate for *Gpx4* loss in endothelial cells *in vivo*.[33] To examine whether this was also the case during reticulocyte maturation and to restrict *Gpx4* deletion to the hematopoietic system, we performed adoptive transfer experiments using bone marrow derived from *Gpx4*$^{F/F}$ or *Mx1-cre/Gpx4*$^{F/F}$ mice. Five weeks after transplantation, mice were kept on a vitamin E-depleted diet (vitE$^{\Delta}$) (7 mg/kg) until the end of the experiment and eight weeks after the transplantation the deletion was induced via poly-I:C (Figure 3A). The mice were sacrificed three weeks after the induction of the deletion. Upon the additional loss of vitamin E, red blood

cell parameters were substantially lower (Figure 3B-D), whereas spleen size and EPO levels further increased (Figure 3F, G). However, dietary vitamin E-depletion caused a significant decrease in reticulocyte numbers in mice that had received *Gpx4*$^{\Delta}$ bone marrow compared to controls (Figure 3E), supporting the notion that under these conditions anemia could no longer be compensated.

Loss of Gpx4 triggers necroptosis

To further examine Gpx4 function in prevention of early erythroid cell death, we employed an erythrocyte maturation model that allows analysis of erythrocyte development *ex vivo*[31]. To initiate erythropoiesis, lineage negative bone marrow cells derived from tamoxifen-inducible *Rosa26-CreERT2/Gpx4*$^{F/F}$ mice[34] were cultured in the presence of erythropoietin and 4-OHT was added 24 hours later to induce loss of *Gpx4*. Upon *Gpx4* deletion the number of viable erythroid cells significantly decreased within 24 hours compared to *Gpx4*$^{F/F}$ control cells (Figure 4A-B, D), which could be prevented by α-tocopherol supplementation as expected (Figure 4D). Flow cytometric analysis confirmed increased cell death (PI^{+} cell number) in *Gpx4*-deficient CD71^{+}Ter119^{+} cells (data not shown). Recently, Gpx4 has been described as an important regulator of ferroptosis[14]. Surprisingly, ferroptosis inhibition using the small inhibitor Fer-1 did not prevent cell death in *Gpx4*$^{\Delta}$ erythroid cultures and even reduced the viability of control cells, whereas erastin and RLS3 induced ferroptosis was completely rescued in control cells and only partially rescued in *Gpx4*$^{\Delta}$ cells using the same concentration (Supplementary Figure 3A). Similarly to Fer-1, another specific ferroptosis inhibitor Lip-1 as well as the iron chelator DFO did not prevent cell death but similarly reduced the number of control cells. Moreover, apoptosis blockade using the pan-caspase inhibitor zVAD did also not improve survival of *Gpx4*$^{\Delta}$ erythroid precursors. However, the RIP1 kinase inhibitor nec-1 normalized cell numbers suggesting that *Gpx4*$^{\Delta}$ erythroid cell death was triggered by necroptosis. Yet, block of TNF signaling by recombinant soluble TNF-RII (etanercept) had no

effect. Because it was recently demonstrated that due to off-target effects nec-1 can prevent death of *Gpx4*-deficient fibroblasts even in the absence of RIP1[17], we aimed to confirm the contribution of necroptosis by genetic ablation of *Rip3*, the upstream kinase responsible for MLKL phosphorylation[35]. To this end we generated *Gpx4*$^{\Delta}$/*Rip3*$^{-/-}$ compound mutants. Loss of GPx4 and RIP3 expression was confirmed by immunoblot analysis (Figure 4E) and indeed *Rip3* deletion prevented *Gpx4*$^{\Delta}$ erythroid cell death (Figure 4F). Flow cytometry confirmed normalization of PI^{+} CD71^{+}Ter119^{+} cells (Figure 4G) and also the number of red colonies was significantly increased in colony assays using bone marrow from *Gpx4*$^{\Delta}$/*Rip3*$^{-/-}$ compound mutants (Figure 4H). In line with these, deletion of *Rip3* also prevented anemia in *Gpx4*$^{\Delta}$ mice *in vivo*. All red cell parameters were normalized (Figure 5A-C) and the number of circulating reticulocytes was significantly decreased in *Gpx4*$^{\Delta}$/*Rip3*$^{-/-}$ mice (Figure 5D). This was paralleled by normalization in both spleen size and serum EPO levels upon loss of *Rip3* in *Gpx4*$^{\Delta}$ mice (Figure 5 E, F). Accordingly, the increased number of TUNEL^{+} cells in *Gpx4*$^{\Delta}$ spleen was significantly reduced in *Gpx4*$^{\Delta}$/*Rip3*$^{-/-}$ double mutants (Fig 5G), which could be further confirmed by flow cytometry (Fig. 5H). Collectively, the data supports the notion that erythroid cells are undergoing RIP3-dependent necroptosis upon oxidative stress caused in the absence of *Gpx4*. Although, Fer-1 addition reduced the ROS accumulation and lipid peroxidation to a significant degree, both parameters were still higher in *Gpx4*$^{\Delta}$ cells compared to controls (Supplementary Figure 3B,C), which sufficed to stabilize RIP1 and RIP3 (Supplementary Figure 3D), explaining ROS induced necroptosis even in the presence of Fer-1.

Necroptosis in Gpx4-deficient erythroid cells is triggered independently of TNFα, CD95 or PARP

Necroptosis is an alternative form of programmed cell death usually associated with elevated levels of ROS[22,36]. Apart from Fas or certain Toll-like-receptor (TLR)

engagement, TNFR signaling is one of the best-characterized triggering events leading to mitochondrial ROS production and necroptosis when caspase-8 is inhibited.[23] Notably, despite having a profound effect on cell survival, *Rip3* deletion did not prevent accumulation of lipid peroxides and ROS in peripheral erythroid cells of *Gpx4*$^{\Delta}$ mice (Figure 6A, B) demonstrating that elevated lipid peroxidation and ROS levels *per se* are not sufficient to induce cell death upon *Gpx4* deletion. Surprisingly, etanercept did not prevent cell death in *Gpx4* deficient erythroid cells *ex vivo* (Figure 4D). In line with these findings, treatment of *Gpx4*$^{\Delta}$ mice with etanercept did not normalize hemoglobin levels or reticulocyte counts (Figure 6C-G, Supplementary Figure 4A). Moreover, also a neutralizing antibody against CD95L at concentrations, which sufficiently block respective signaling *in vivo* (Supplementary Figure 4B-D), did not normalize anemia or compensatory reticulocytosis (Figure 6 C-G) excluding the role of both TNFR and FAS signaling as upstream events in necroptosis of *Gpx4* deficient erythroid cells. Furthermore, despite a marked accumulation of phospho-H2A.X^{+} foci in the spleens of *Gpx4*$^{\Delta}$ mice (Figure 6 H-J), PARP inhibition, which is known to block genotoxic stress-triggered necroptosis[23], did not prevent anemia (Figure 6 K-O, Supplementary Figure S4F-H). Collectively, these data suggested that necroptosis was triggered independently of the classical activation pathways. In order to test whether loss of *Gpx4* led to the formation of the necrosome we performed immunoprecipitation assays using protein lysates from *in vitro* differentiated erythroid cells. Indeed, 4-OHT induced *Gpx4* loss triggered interaction of caspase 8 and RIP1, however, we were not able to detect any recruitment of FADD to this complex (Figure 7A). Yet, FADD was sufficiently recruited when necroptosis was triggered by TNFα in the absence of caspase and TAK activity in the presence of Gpx4 (Figure 7A) supporting the notion that Gpx4 dependent necroptosis in erythroid cells occurred independently of TNFα activation. Caspase 8 comprises an important inhibitor of the necrosome being responsible for direct

cleavage of RIP1 and RIP3[22] as well as of the RIP1 activating deubiquitinase CYLD.[37] Thus, lack of caspase 8 function is associated with induction of necroptosis. Therefore, we reasoned that caspase 8 function might be impaired in *Gpx4*$^{\Delta}$ cells despite its recruitment and interaction with RIP1. This was confirmed as cleavage of caspase 8 was impaired in *Gpx4*$^{\Delta}$ *in vitro* differentiated erythrocytes when treated with TNFα in the presence of the TAK1 inhibitor 5Z-7-Oxozeaenol (TAKi) (Figure 7B). Shifting the redox potential towards oxidation has recently been demonstrated to decrease caspase 1 activity by transient glutathionylation.[38] To examine whether the increased ROS production caused by *Gpx4* deficiency might similarly affect caspase 8 function in *Gpx4*$^{\Delta}$ cells, we checked the glutathione state in CD71^{+}/Ter119^{+} erythroid progenitor cells isolated from bone marrow. As expected, *Gpx4* loss caused a dramatic increase in oxidized glutathione (GSSG) leading to a decrease in the ratio of reduced to oxidized glutathione (GSH/GSSG) (Figure 7C, D). Moreover, when the CD71^{+}/Ter119^{+} erythroid progenitor cells were loaded with biotin-labeled glutathione ethylester (BioGEE) to precipitate glutathionylated proteins, immunoblot analysis of caspase 8 showed a marked glutathionylation in *Gpx4*$^{\Delta}$ cells compared to controls (Fig. 7E). Consequently, in *in vitro* cultured progenitor cells DTT prevented necrotic cell death and prevented caspase 8 inhibition (Fig. 7F, G), yet this was not due to DTT-dependent inhibition of lipid peroxidation or ROS accumulation (Fig. 7H, I). Collectively, these results indicate that in *Gpx4*$^{\Delta}$ cells although caspase 8 is readily recruited to the necrosome, its functional impairment due to glutathionylation results in necrotic cell death.

Discussion

Erythrocytes are well equipped with a variety of antioxidant systems to scavenge oxidative stress. So far, Gpx4, one of the most important mammalian redox enzymes, has not been considered to be part of this finely tuned anti-oxidant defense system in this cell lineage. Here we show that Gpx4 plays an important role in

scavenging ROS and lipid hydroperoxides in the erythroid lineage. Loss of Gpx4 causes erythroid precursor cell death, which results in the development of anemia. However, this can be partially compensated in the presence of exogenous vitamin E, while in the absence of vitamin E supplementation compensatory reticulocytosis is completely impaired. Thus, vitamin E acts as the compensating ROS scavenger and provides a back-up system for Gpx4 *in vivo* as it has recently been suggested in endothelial cells[33]. Similar kinetics of biotin labeled Ter119^{+} cells underscore the notion that *Gpx4*$^{\Delta}$ mice do not develop hemolytic anemia but are rather characterized by insufficient erythropoiesis.

Lipid peroxidation, ROS formation and induction of necrosis have been linked to an increase in redox-active iron, the so called intracellular labile iron pool (LIP), by several groups[39-42] and to an increase in lysosomal iron.[43] Recently, a novel form of cell death, termed ferroptosis, has been described. Ferroptosis is triggered by the lethal oncogenic Ras-selective small molecule erastin in cancer cells in an iron-dependent fashion and could not be inhibited by nec-1.[15] In fact, recent data suggested an important role of Gpx4 for the survival of T cells and renal tubular cells by preventing ferroptosis.[14] Here we provide evidence that in erythroid cells Gpx4 rather suppresses Rip3-dependent necroptosis. Although the cell death mechanisms seems to vary between different cell types, Gpx4 is clearly a vital element for the homeostasis of hematopoietic cells via regulating the cellular redox balance and thus inhibiting cell death. However, it is not clear to what extent these different cell death pathways are overlapping or interchangeable based on genetic or environmental alterations. There are several studies demonstrating the complex interchange between death mechanisms upon genetic alterations of the regulating elements such as FADD, caspase 8, RIP1 and RIP3.[44-46]

Different subcellular sources of ROS have been described to contribute to TNFα- induced necrosis in L929 cells. ROS produced at complex I and II in the mitochondrial electron transport chain play a crucial role in the execution of TNFα-

induced necrosis.[39] Anti-oxidants as well as iron chelators were able to rescue L929 cells from TNFα-induced necrosis implying that the intracellular labile iron pool and ROS generated through the Fenton reaction play an important role in the execution of cell death.[39] Engagement of TNFR1 by TNF induces formation of a signaling complex consisting of TRADD, RIP1 and the NADPH oxidase Nox1 that leads to Nox1 activation, O2- production at the plasma membrane, long term JNK1 activation by cytoplasmic ROS and necrotic cell death.[40,41] Furthermore, TNFα can stimulate ROS formation by favoring JNK1-dependent degradation of ubiquitous iron-binding protein ferritin leading to an increase in redox-active iron.[42] Importantly, however, in all instances ROS and lipid peroxidation have been considered essential downstream effectors of RIP1/RIP3 dependent signaling. Yet, we show here that deletion of *Rip3* prevents anemia induced by *Gpx4* deletion without inhibiting lipid peroxidation and ROS production thereby suggesting lipid peroxides and ROS can act as signaling molecules upstream of the necrosome independently of TNFα stimulation. However, this does not rule out the possibility that ROS may also play an important role as effectors of necrotic cell death downstream of the RIP/RIP3 signaling complex. Indeed, the slight reduction in lipid peroxidation and ROS levels upon additional deletion of *Rip3* is possibly verifying the role of cellular ROS induction during the execution of RIP3 dependent necroptosis even though the necroptosis in the case of Gpx4 deficiency is independent of TNFR signaling. Consistent with a lack of FADD recruitment to the necrosome complex neither TNFα nor FAS ligand as well as DNA damage dependent PARP1 activation play a role in the induction of Gpx4-deficient cell death. Thus, we propose a so far unrecognized unconventional pathway for the initiation of necroptosis, independently of TNFR and FAS engagement. One important prerequisite seems to be the functional inactivation of caspase 8 possibly by glutathionylation in *Gpx4* deficient cells. Similarly, glutathionylation has been proposed to be involved in the regulation of caspase 1 and caspase 3.[38,47] Because glutathionylation is a direct consequence of oxidation,

our findings may nevertheless also be relevant for classical TNFα dependent necrosome activation as ROS that are formed downstream of RIP1/RIP3 may interfere with caspase 8 activity and therefore fuel into a feed-forward loop.[44] Furthermore, we cannot rule out that caspase 8 is also inhibited by direct oxidation of the active-site cysteine.[49,50]

In conclusion, our data provide direct genetic evidence that Gpx4 can act as a yet unrecognized regulator of RIP3 dependent necroptosis in a cell type dependent manner. The underlying explanation for this particular cell type specific difference is currently unknown but it will be important to identify the factors that determines the cell death mechanism - necroptosis versus ferroptosis - when Gpx4 is not functional.

Acknowledgements

We thank Natalia Delis, Christin Danneil, Eva Rudolf, Kerstin Burmeister and Saskia Ettl for expert technical assistance. We are grateful to Vishva Dixit and Kim Newton for providing *Rip3*$^{-/-}$ mice as well as Markus Conrad for providing *Gpx4*$^{F/F}$ mice. This work was supported in part by the LOEWE Center for Cell and Gene Therapy Frankfurt (CGT, III L 4-518/17.004) and institutional funds from the Georg-Speyer-Haus, as well as a grant from the European Research Council (ERC 281967).

Author contributions

Ö.C., Y.B.A., N.V., L.H., P.S.H., performed and together with T.S., G.W.B. and F.R.G. analyzed experiments. S.G. and P.V. contributed to the analysis of cell death. G.W.B. and F.R.G supervised and designed the experiments and together with Ö.C. wrote the manuscript.

Conflict-of-interest disclosure: The authors declare no competing financial interests.

References

1. D'Autréaux B, Toledano MB. ROS as signalling molecules: mechanisms that generate specificity in ROS homeostasis. *Nat Rev Mol Cell Biol*. 2007;8(10):813–24.
2. Vanden Berghe T, Vanlangenakker N, Parthoens E, et al. Necroptosis, necrosis and secondary necrosis converge on similar cellular disintegration features. *Cell Death Differ*. 2010;17(6):922– 30.
3. Fiers W, Beyaert R, Declercq W, Vandenabeele P. More than one way to die: apoptosis, necrosis and reactive oxygen damage. *Oncogene*. 1999;18(54):7719–30.
4. Beutler E, Luzzatto L. Hemolytic anemia. *Semin Hematol*. 1999;36(4 Suppl 7):38–47.
5. Johnson RM, Ho Y-S, Yu D-Y, et al. The effects of disruption of genes for peroxiredoxin-2, glutathione peroxidase-1, and catalase on erythrocyte oxidative metabolism. *Free Radic Biol Med*. 2010;48(4):519–25.
6. Lee TH, Kim SU, Yu SL, et al. Peroxiredoxin II is essential for sustaining life span of erythrocytes in mice. *Blood*. 2003;101(12):5033–8.
7. Neumann CA, Krause DS, Carman CV, et al. Essential role for the peroxiredoxin Prdx1 in erythrocyte antioxidant defence and tumour suppression. *Nature*. 2003;424(6948):561–5.
8. Kaushal N, Hegde S, Lumadue J, Paulson RF, Prabhu KS. The regulation of erythropoiesis by selenium in mice. *Antioxid Redox Signal*. 2011;14(8):1403–12.
9. Behne D, Kyriakopoulos A. Mammalian selenium-containing proteins. *Annu Rev Nutr*. 2001;21:453–73.
10. Imai H, Hirao F, Sakamoto T, et al. Early embryonic lethality caused by targeted disruption of the mouse PHGPx gene. *Biochem Biophys Res Commun*. 2003;305(2):278–86.

11. Yant LJ, Ran Q, Rao L, et al. The selenoprotein GPX4 is essential for mouse development and protects from radiation and oxidative damage insults. *Free Radical Biology and Medicine*. 2003;34(4):496–502.
12. Seiler A, Schneider M, Förster H, et al. Glutathione peroxidase 4 senses and translates oxidative stress into 12/15-lipoxygenase dependent- and AIF-mediated cell death. *Cell Metab*. 2008;8(3):237–48.
13. Ueta T, Inoue T, Furukawa T, et al. Glutathione peroxidase 4 is required for maturation of photoreceptor cells. J Biol Chem. 2012;287(10):7675–82.
14. Matsushita M, Freigang S, Schneider C, et al. T cell lipid peroxidation induces ferroptosis and prevents immunity to infection. *J Exp Med.* 2015;212(4):555–568.
15. Dixon SJ, Lemberg KM, Lamprecht MR, et al. Ferroptosis: an iron- dependent form of nonapoptotic cell death. *Cell*. 2012;149(5):1060– 72.
16. Yang WS, SriRamaratnam R, Welsch ME, et al. Regulation of ferroptotic cancer cell death by GPX4. *Cell*. 2014;156(1-2):317–31.
17. Friedmann Angeli JP, Schneider M, Proneth B, et al. Inactivation of the ferroptosis regulator Gpx4 triggers acute renal failure in mice. *Nat Cell Biol*. 2014;16(12):1180–91.
18. Bergsbaken T, Fink SL, Cookson BT. Pyroptosis: host cell death and inflammation. *Nat Rev Microbiol*. 2009;7(2):99–109.
19. Christofferson DE, Yuan J. Necroptosis as an alternative form of programmed cell death. *Curr Opin Cell Biol*. 2010;22(2):263–8.
20. Wang Y, Dawson VL, Dawson TM. Poly(ADP-ribose) signals to mitochondrial AIF: a key event in parthanatos. *Exp Neurol*. 2009;218(2):193–202.
21. Degterev A, Hitomi J, Germscheid M, et al. Identification of RIP1 kinase as a specific cellular target of necrostatins. *Nat Chem Biol*. 2008;4(5):313–21.

22. Vandenabeele P, Galluzzi L, Vanden BT, Kroemer G. Molecular mechanisms of necroptosis: an ordered cellular explosion. *Nat Rev Mol Cell Biol*. 2010;11(10):700–14. □

23. Han J, Zhong CQ, Zhang DW. Programmed necrosis: backup to and competitor with apoptosis in the immune system. *Nat Immunol*. 2011;12(12):1143–9. □

24. Kaiser W, Upton J, Long A, et al. RIP3 mediates the embryonic lethality of caspase-8-deficient mice. *Nature*. 2011;471(7338):368– 72. □

25. Oberst A, Dillon CP, Weinlich R, et al. Catalytic activity of the caspase-8-FLIP(L) complex inhibits RIPK3-dependent necrosis. *Nature*. 2011;471(7338):363–7. □

26. Zhang H, Zhou X, McQuade T, et al. Functional complementation between FADD and RIP1 in embryos and lymphocytes. *Nature*. 2011;471(7338):373–6.

27. Welz P, Wullaert A, Vlantis K, et al. FADD prevents RIP3-mediated epithelial cell necrosis and chronic intestinal inflammation. *Nature*. 2011; 477(7364):330-4. □

28. Bonnet MC, Preukschat D, Welz P-S, et al. The adaptor protein FADD protects epidermal keratinocytes from necroptosis in vivo and prevents skin inflammation. *Immunity*. 2011;35(4):572–82. □

29. Dillon CP, Oberst A, Weinlich R, et al. Survival function of the FADD-CASPASE-8-cFLIP(L) complex. *Cell Rep*. 2012;1(5):401–7. □

30. Newton K, Sun X, Dixit VM. Kinase RIP3 Is Dispensable for Normal NF- Bs, Signaling by the B-Cell and T-Cell Receptors, Tumor Necrosis Factor Receptor 1, and Toll-Like Receptors 2 and 4. *Molecular and Cellular Biology*. 2004;24(4):1464–1469.

31. Shuga J, Zhang J, Samson LD, Lodish HF, Griffith LG. In vitro erythropoiesis from bone marrow-derived progenitors provides a physiological assay for

toxic and mutagenic compounds. *Proc Natl Acad Sci U S A*. 2007;104(21):8737–42.

32. Kühn R, Schwenk F, Aguet M, Rajewsky K. Inducible gene targeting in mice. *Science*. 1995;269(5229):1427–9.
33. Wortmann M, Schneider M, Pircher J, et al. Combined deficiency in glutathione peroxidase 4 and vitamin E causes multiorgan thrombus formation and early death in mice. *Circ Res*. 2013;113(4):408–17.
34. Hameyer D, Loonstra A, Eshkind L, et al. Toxicity of ligand- dependent Cre recombinases and generation of a conditional Cre deleter mouse allowing mosaic recombination in peripheral tissues. *Physiol Genomics*. 2007;31(1):32–41.
35. Silke J, Rickard JA, Gerlic M. The diverse role of RIP kinases in necroptosis and inflammation. *Nat Immunol*. 2015;16(7):689–697.
36. Degenhardt K, Mathew R, Beaudoin B, et al. Autophagy promotes tumor cell survival and restricts necrosis, inflammation, and tumorigenesis. *Cancer Cell*. 2006;10(1):51–64.
37. O'Donnell MA, Perez-Jimenez E, Oberst A, et al. Caspase 8 inhibits programmed necrosis by processing CYLD. *Nat Cell Biol*. 2011;13(12):1437–42.
38. Meissner F, Molawi K, Zychlinsky A. Superoxide dismutase 1 regulates caspase-1 and endotoxic shock. *Nat Immunol*. 2008;9(8):866–72.
39. Schulze-Osthoff K, Bakker AC, Vanhaesebroeck B, et al. Cytotoxic activity of tumor necrosis factor is mediated by early damage of mitochondrial functions. Evidence for the involvement of mitochondrial radical generation. *J Biol Chem*. 1992;267(8):5317– 23.
40. Kamata H, Honda S, Maeda S, et al. Reactive oxygen species promote TNFalpha-induced death and sustained JNK activation by inhibiting MAP kinase phosphatases. *Cell*. 2005;120(5):649–61.

41. Kim Y, Morgan M, Choksi S, Liu Z. TNF-induced activation of the Nox1 NADPH oxidase and its role in the induction of necrotic cell death. *Mol Cell*. 2007;26(5):675–87. □

42. Xie C, Zhang N, Zhou H, et al. Distinct roles of basal steady-state □and induced H-ferritin in tumor necrosis factor-induced death in □L929 cells. *Mol Cell Biol*. 2005;25(15):6673–81. □

43. Berndt C, Kurz T, Selenius M, et al. Chelation of lysosomal iron protects against ionizing radiation. *Biochem J*. 2010;432(2):295– 301.

44. Dannappel M, Vlantis K, Kumari S, et al. RIPK1 maintains epithelial homeostasis by inhibiting apoptosis and necroptosis. *Nature*. 2014;513(7516):90–4. □

45. Takahashi N, Vereecke L, Bertrand MJM, et al. RIPK1 ensures intestinal homeostasis by protecting the epithelium against apoptosis. *Nature*. 2014;513(7516):95–9.

46. Rickard JA, O'Donnell JA, Evans JM, et al. RIPK1 regulates RIPK3-MLKL-driven systemic inflammation and emergency hematopoiesis. *Cell*. 2014;157(5):1175–88. □

47. Pan S, Berk BC. Glutathiolation regulates tumor necrosis factor- alpha-induced caspase-3 cleavage and apoptosis: key role for glutaredoxin in the death pathway. *Circ Res*. 2007;100(2):213–9. □

48. Goossens V, De Vos K, Vercammen D, et al. Redox regulation of TNF signaling. *Biofactors*. 1999;10(2-3):145–56. □

49. Borutaite V, Brown GC. Caspases are reversibly inactivated by hydrogen peroxide. *FEBS Lett*. 2001;500(3):114–8. □

50. Hampton MB, Stamenkovic I, Winterbourn CC. Interaction with substrate sensitises caspase-3 to inactivation by hydrogen peroxide. *FEBS Lett*. 2002;517(1-3):229–32. □□

51. Socolovsky M, Nam H, Fleming M, et al. Ineffective erythropoiesis in Stat5a$^{-/-}$ 5b$^{-/-}$ mice due to decreased survival of early erythroblasts. *Blood*. 2001;98(12):3261.

Figure legends

Figure 1: Loss of *Gpx4* in hematopoietic cells induces anemia that is compensated by increased erythropoiesis. (A) Immunoblot analysis of Gpx4 in peripheral erythrocytes (TER119$^+$) and bone marrow erythroid progenitors (CD71$^+$/TER119$^+$). (B-E) Red blood cell counts (B), hemoglobin (C) and hematocrit (D) levels are decreased in *Gpx4*$^\Delta$ mice whereas the number of reticulocytes is increased (E). Data are mean ± SE; n≥20; *** p <0.001 by t-test. (F) Elevated serum erythropoietin (EPO) levels and enlarged spleens (G) in *Gpx4*$^\Delta$ mice. Data are mean ± SE; n≥10; ** p < 0.01, *** p < 0.001 by t-test. (H, I) Immunohistochemistry staining of BrdU incorporation in the spleen. Image acquisition was performed using Zeiss Axio Imager M2 with x20/0.5 EC Plan Neofluar objective. (J) Quantification of splenic BrdU$^+$/TER119$^+$ cells determined by flow cytometry. Data are mean ± SE; n≥3; *** p < 0.001 by t-test.

Figure 2: Increased lipid peroxidation and oxidative stress in *Gpx4*$^\Delta$ erythroid cells does not impair their life span in the periphery. (A) Measurement of lipid peroxidation in unchallenged peripheral TER119$^+$ erythrocytes using lipophilic redox-sensitive dye BODIPY 581/591, which upon oxidation shifts its fluorescence from red to green. Data are mean ± SE; n≥7; * p < 0.05 by t-test. (B) ROS in unchallenged peripheral TER119$^+$ erythrocytes using redox- sensitive dye CM-H_2-DCFDA. n≥7; * p < 0.05 by t-test. (C) Survival of biotin labeled peripheral TER119$^+$ erythrocytes. Data are mean ± SE; n≥6. (D) Increased number of peripheral CD71$^+$/TER119$^+$ reticulocytes in *Gpx4*$^\Delta$ mice within the first 4 weeks after poly-I:C administration. Data are mean ± SE; n≥5; * p < 0.05, ** p < 0.01 by t-test. (E-F) Representative images of TUNEL assay in spleen sections showing increased cell death in *Gpx4*$^\Delta$ mice. Image acquisition was performed using Zeiss Axio Imager M2 with x40/0.95 korr. Apochromat objective. (G-H) Flow cytometry analysis using propidium iodide (PI) to determine the number of non-viable CD71$^+$ cells in bone marrow (G) and in spleen

(H). Data are mean ± SE; n≥3; * $p < 0.05$ by t-test. (I) Formation of o-dianisidine-positive erythroid colonies from bone marrow in methylcellulose semisolid media. Red colony formation of *Gpx4*$^{\Delta}$ bone marrow cells could be rescued by addition of α-tocopherol to the medium. Data are mean ± SE; n≥3; *** $p < 0.001$ by t-test; **n.s.**: not significant.

Figure 3: Increased erythropoiesis in *Gpx4*$^{\Delta}$ mice depends on vitamin E. (A) Schematic overview of treatment: bone marrow from *Gpx4*$^{F/F}$ or *Mx1Cre*/*Gpx4*$^{F/F}$ mice was transplanted (BMT) into wild type recipients, the mice were kept on a vitamin E-depleted diet (vitE$^{\Delta}$) after the recovery and deletion was induced by poly I:C. (B-E) Red blood cell number (B), hemoglobin (C) and hematocrit (D) levels as well as reticulocyte counts (E). Data are mean ± SE; n≥4; *** $p < 0.001$, * $p < 0.05$ by t-test. (F, G) Enlarged spleens (F) and elevated serum EPO levels (G) in transplanted mice. Data are mean ± SE; n≥6; *** $p < 0.001$, ** $p < 0.01$, * $p < 0.05$ by t-test.

Figure 4: RIP3-dependent necroptosis but not ferroptosis causes cell death in *Gpx4* deficient erythroid progenitor cells. Erythroid cells were differentiated *in vitro* from *Gpx4*$^{F/F}$ and *Rosa26-Cre*ER^{T2}/*Gpx4*$^{F/F}$ bone marrow and deletion was induced by 4-OHT after 24 hours of culture in the presence of EPO. (A-B) Microscopic images of *in vitro* differentiated erythroid cells from *Gpx4*$^{F/F}$ (A) and *Rosa26-Cre*ER^{T2}/*Gpx4*$^{F/F}$ (B) bone marrow 48 hours after the induction of deletion with tamoxifen. (C) Schematic illustration of programmed cell death pathways. Ferroptosis is triggered by an iron dependent accumulation of lethal ROS and lipid peroxides in cells, which can be inhibited via iron chelators, such as DFO. Ferroptosis can be induced by erastin, which inhibits cellular cysteine uptake and thus limiting the production of intracellular GSH or by RSL-3 via inhibition of GPx4 leading to increased lipid peroxidation and ROS accumulation. Fer-1 and liproxstatin-1 inhibits ferroptosis via inhibiting the lipid peroxidation. Apoptosis and necroptosis

are mainly regulated via TNFR1 signaling. Upon TNF binding, TNFR1 undergoes a conformational change, activating two possible cell death execution mechanisms: caspase dependent or caspase independent. Normaly, caspase 8 triggers apoptosis by activating the classical caspase cascade. It also cleaves, and hence inactivates, RIP1 and RIP3. If caspase 8 is inhibited (e.g. via zVAD), phosphorylated RIP1 and RIP3 engage the effector mechanisms of necroptosis. (D) Percentage of viable *in vitro* differentiated erythroid cells counted via trypan blue exclusion 48 hours after the induction of deletion in the presence of α-Toc, the most prominent member of the vitamin E family, ferroptosis inhibitor Fer-1 and Lip-1, iron chelator DFO, pan-caspase inhibitor zVAD, RIP1 kinase inhibitor nec-1, or recombinant sTNFRII (etanercept). Data are mean ± SE; n≥6; * $p < 0.05$ by t-test. (E) Absence of Gpx4 and RIP3 is verified by immunoblot analysis. (F) Percentage of viable *in vitro* differentiated erythroid cells from *Gpx4*$^{F/F}$, *Rip3*$^{-/-}$, *Rosa26-Cre*ER^{T2}/*Gpx4*$^{F/F}$ and *Rip3*$^{-/-}$/*Rosa26-Cre*ER^{T2}/*Gpx4*$^{F/F}$ 48 hours after the induction of deletion. Data are mean ± SE; n≥8; *** $p < 0.001$ by ANOVA /Bonferroni. (G) Flow cytometry analysis of *in vitro* cultured erythroid cells 36 hours after the 4-OHT treatment to analyze necrotic cells (AnnexinV^{-}PI^{+}). Data are mean ± SE; n≥4; * $p < 0.05$ by ANOVA/Bonferroni. (H) Deletion of *Rip3* significantly improved the formation of erythroid o-dianisidine-positive *Gpx4*$^{\Delta}$ colonies similar to α-Toc supplementation. Data are mean ± SE; n≥3; * $p<0.05$, ** $p < 0.01$, *** $p < 0.001$ by ANOVA/Bonferroni. n.s.: not significant.

Figure 5: Genetic deletion of *Rip3* normalizes red cell parameters and rescues anemia. (A-D) Normalization of red blood cells (A), hemoglobin levels (B), hematocrit (C), reduction of reticulocyte numbers (D). (E-F) Elevated serum EPO levels (E) and enlarged spleens (F) in *Gpx4*$^{\Delta}$ mice are normalized upon deletion of *Rip3*. Data are mean ± SE; n≥9; * $p < 0.05$, ** $p < 0.01$, *** $p < 0.001$ by ANOVA/Bonferroni. (G) Quantification of TUNEL^{+} cells in the spleen sections. (H)

Flow cytometry analysis of AnnexinV$^-$PI$^+$ erythroid progenitor cells in the spleen. Data are mean ± SE; n≥4; ** p < 0.01 by ANOVA/Bonferroni.

Figure 6: Necroptosis in *Gpx4*$^{\Delta}$ mice is triggered independently of TNFR or CD95 engagement and PARP activation. (A-B) Lipid peroxidation (A) and ROS accumulation (B) in the peripheral blood erythroid cells TER119$^+$ are not significantly affected upon *Rip3* deletion. Data are mean ± SE; n≥4; * p < 0.05, ** p < 0.01, *** p < 0.001 by ANOVA/Bonferroni. (C-G) The number of peripheral CD71$^+$/TER119$^+$ cells remains unaffected (C), no change in red blood cells (D), hemoglobin (E), hematocrit (F) and reticulocytes (G) in *Gpx4*$^{\Delta}$ mice when treated with etanercept (5mg/kg) or α-CD95L neutralizing antibody (50µg) for two weeks. Data are mean ± SE; n≥5 **n.s.**: not significant. (H-J) Immunohistochemistry of phospho-H2Ax in the spleen (H,I) and the quantification of phospho-H2Ax$^+$ foci (J). Data are mean ± SE; n≥3; *** p < 0.001 by t-test. (K-O) The number of peripheral CD71$^+$/TER119$^+$ cells remains unaffected (K), no change in red blood cells (L), hemoglobin (M), hematocrit (N) and reticulocytes (O) in *Gpx4*$^{\Delta}$ mice when treated with PARP inhibitor olaparib (5mg/kg) for two weeks. Data are mean ± SE; n≥5. n.s.: not significant.

Figure 7: Caspase 8 is inactivated in *Gpx4* deficient cells

(A) Immunoprecipitation (IP) of caspase 8 and immunoblot analysis of RIP1 and FADD in *in vitro* erythroid cultures which are treated with 4-OHT for 36 hours. Classical activation of necroptosis using zVAD/TAKi/TNFα treatment in wild type *in vitro* cultured erythroid cells shows a strong interaction of caspase 8 with RIP1 and FADD upon two hours of stimulation. (B) Cleavage of caspase 8 is blocked in *in vitro* cultured *Gpx4*$^{\Delta}$ erythroid cells 36 hours after 4-OHT treatment determined by immunoblot of caspase 8 when stimulated 2 hours with TNFα in the presence of TAK inhibitor 5Z-7- Oxozeaenol (TAKi) while zVAD treatment completely inhibits caspase 8 cleavage. (C, D) Concentration of oxidized glutathione (GSSG) (C) and ratio of

reduced to oxidized glutathione (GSH/GSSG) (D) in peripheral blood cells of *Gpx4*$^{\Delta}$ mice and control littermates. (E) Detection of glutathionylated caspase 8 in peripheral CD71^{+}/TER119^{+} cells from *Gpx4*$^{\Delta}$ mice. Cells were loaded with BioGEE and immunoblot analysis was performed after immunoprecipitation (IP) with streptavidin (strep). Data shown is representative of four independently analyzed mice of each genotype. (F, G) DTT supplementation rescues cell death in erythroid cells (F) and restores caspase 8 cleavage upon TNFα stimulation (G). (H, I) DTT treatment does not inhibit lipid peroxidation (H) or ROS accumulation in cultured erythroid cells of either genoytpe (I). (J) Our model proposes that in the absence of GPx4, lipid peroxides and ROS can act as signaling molecules upstream of the necrosome independently of TNFR/FAS signaling. Loss of GPx4 in erythroid lineage leads to inactivation of caspase 8 via glutathionylation. ROS and lipid peroxides activate RIP1/RIP3 containing necrosome and trigger necroptotic cell death. Presence of vitamin E can compensate Gpx4 deficiency.

Figure 1

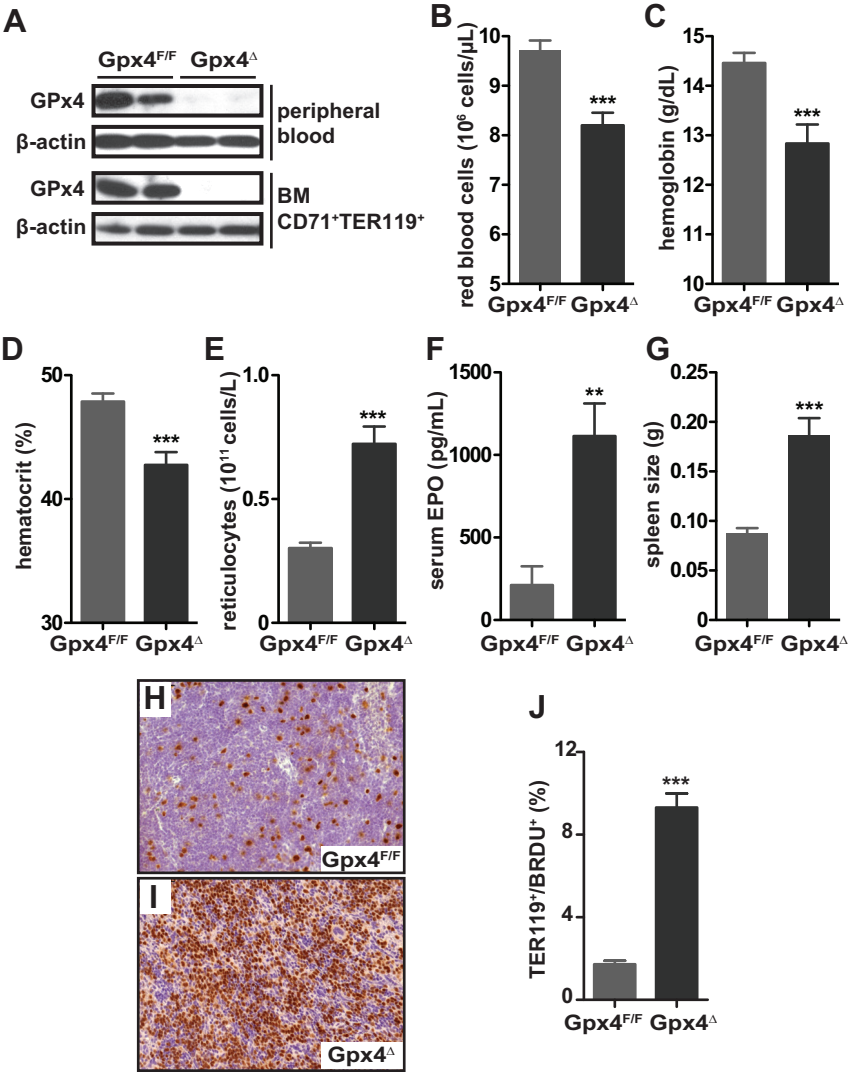
A
Gpx4F/F
Gpx4Δ
GPx4
β-actin
peripheral blood
GPx4
β-actin
BM CD71+TER119+
B
red blood cells (10^6 cells/μL)
10
9
8
7
6
5
***
Gpx4F/F
Gpx4Δ
C
hemoglobin (g/dL)
15
14
13
12
11
10
***
Gpx4F/F
Gpx4Δ
D
hematocrit (%)
50
40
30
***
Gpx4F/F
Gpx4Δ
E
reticulocytes (10^11 cells/L)
1.0
0.5
0
***
Gpx4F/F
Gpx4Δ
F
serum EPO (pg/mL)
1500
1000
500
0
**
Gpx4F/F
Gpx4Δ
G
spleen size (g)
0.25
0.20
0.15
0.10
0.05
0
***
Gpx4F/F
Gpx4Δ
H
Gpx4F/F
I
Gpx4Δ
J
TER119+/BRDU+ (%)
12
8
4
0
***
Gpx4F/F
Gpx4Δ

Figure 2

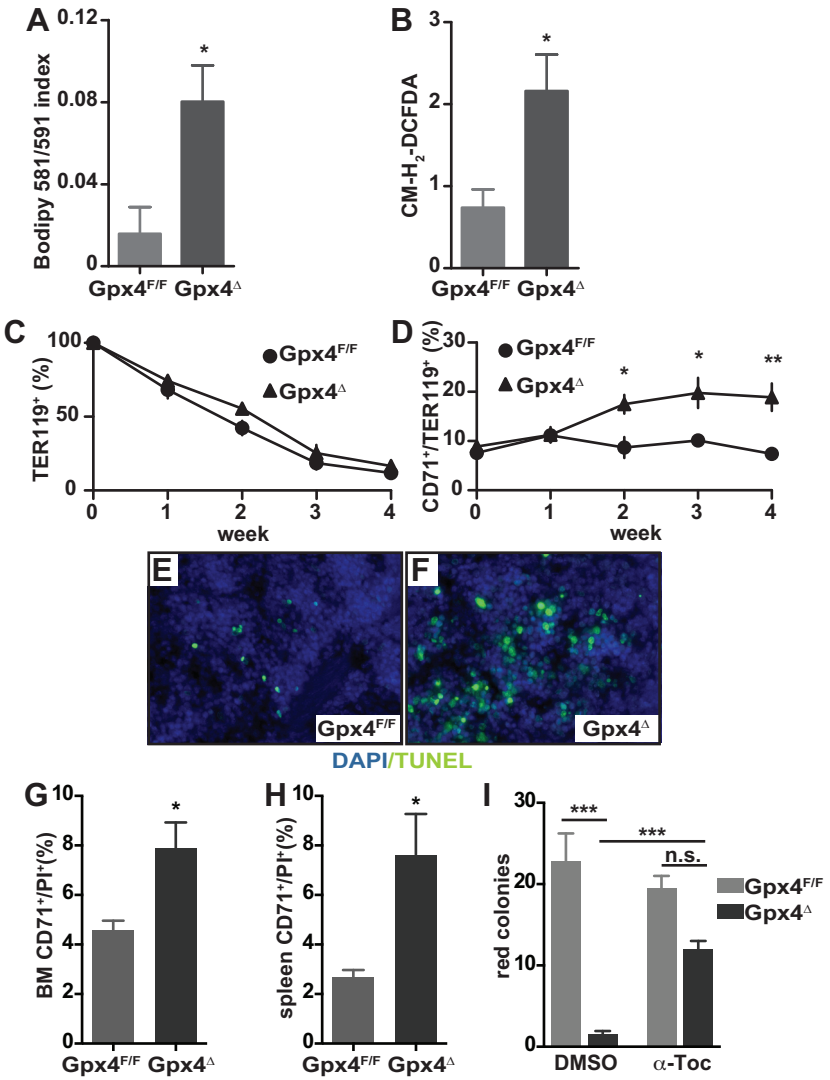
A
Bodipy 581/591 index
0.12
0.08
0.04
0
*
Gpx4F/F
Gpx4Δ
B
CM-H2-DCFDA
3
2
1
0
*
Gpx4F/F
Gpx4Δ
C
TER119+ (%)
100
50
0
Gpx4F/F
Gpx4Δ
0
1
2
3
4
week
D
CD71+/TER119+ (%)
30
20
10
0
Gpx4F/F
Gpx4Δ
*
*
**
0
1
2
3
4
week
E
Gpx4F/F
F
Gpx4Δ
DAPI/TUNEL
G
BM CD71+/PI+(%)
10
8
6
4
2
0
*
Gpx4F/F
Gpx4Δ
H
spleen CD71+/PI+(%)
10
8
6
4
2
0
*
Gpx4F/F
Gpx4Δ
I
red colonies
30
20
10
0
***
***
n.s.
Gpx4F/F
Gpx4Δ
DMSO
α-Toc

Figure 3

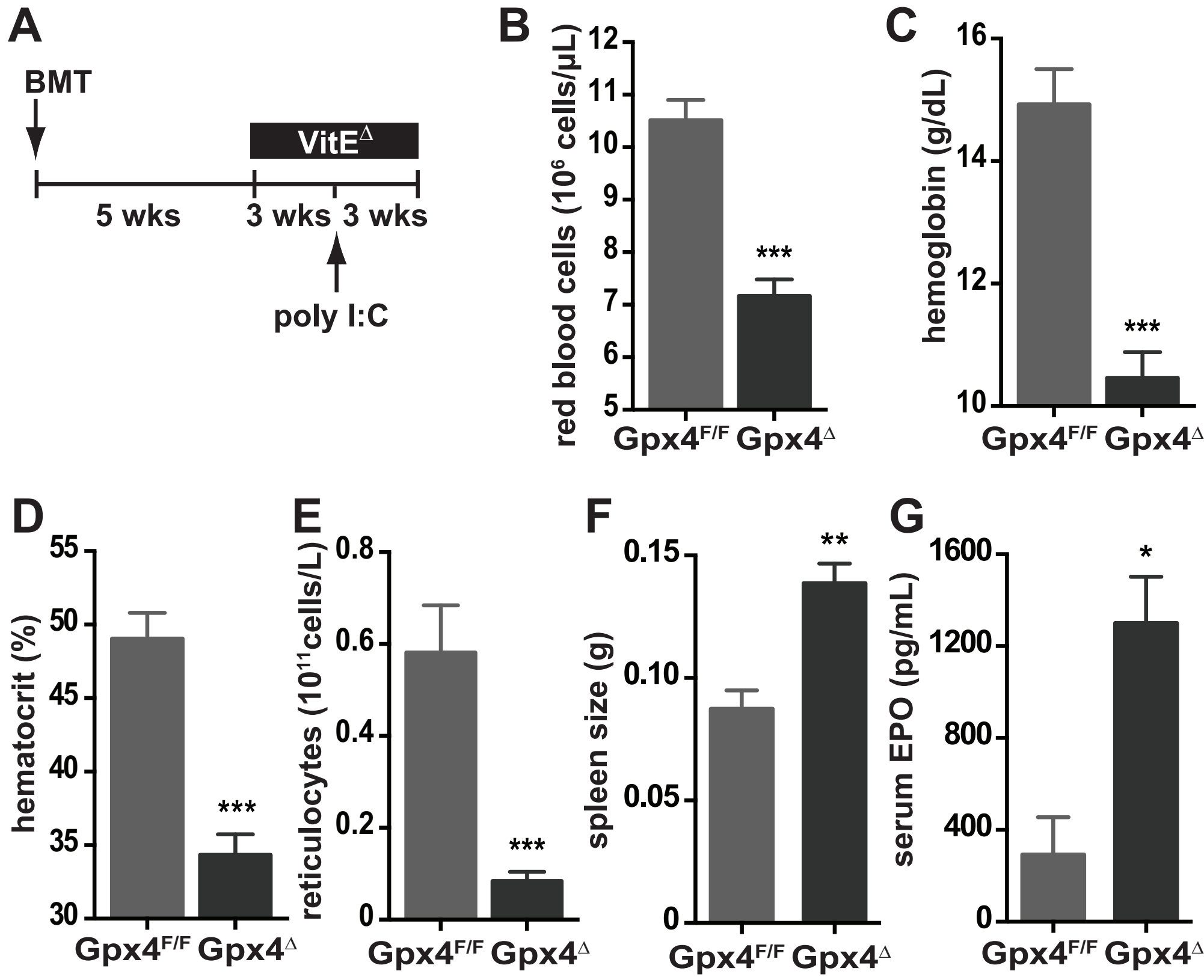
A
BMT
VitE$^{\Delta}$
5 wks
3 wks
3 wks
poly I:C
B
red blood cells (10^6 cells/µL)
12
11
10
9
8
7
6
5
***
Gpx4$^{F/F}$
Gpx4$^{\Delta}$
C
hemoglobin (g/dL)
16
14
12
10
***
Gpx4$^{F/F}$
Gpx4$^{\Delta}$
D
hematocrit (%)
55
50
45
40
35
30
***
Gpx4$^{F/F}$
Gpx4$^{\Delta}$
E
reticulocytes (10^{11}cells/L)
0.8
0.6
0.4
0.2
0
***
Gpx4$^{F/F}$
Gpx4$^{\Delta}$
F
spleen size (g)
0.15
0.10
0.05
0
**
Gpx4$^{F/F}$
Gpx4$^{\Delta}$
G
serum EPO (pg/mL)
1600
1200
800
400
0
*
Gpx4$^{F/F}$
Gpx4$^{\Delta}$

Figure 4

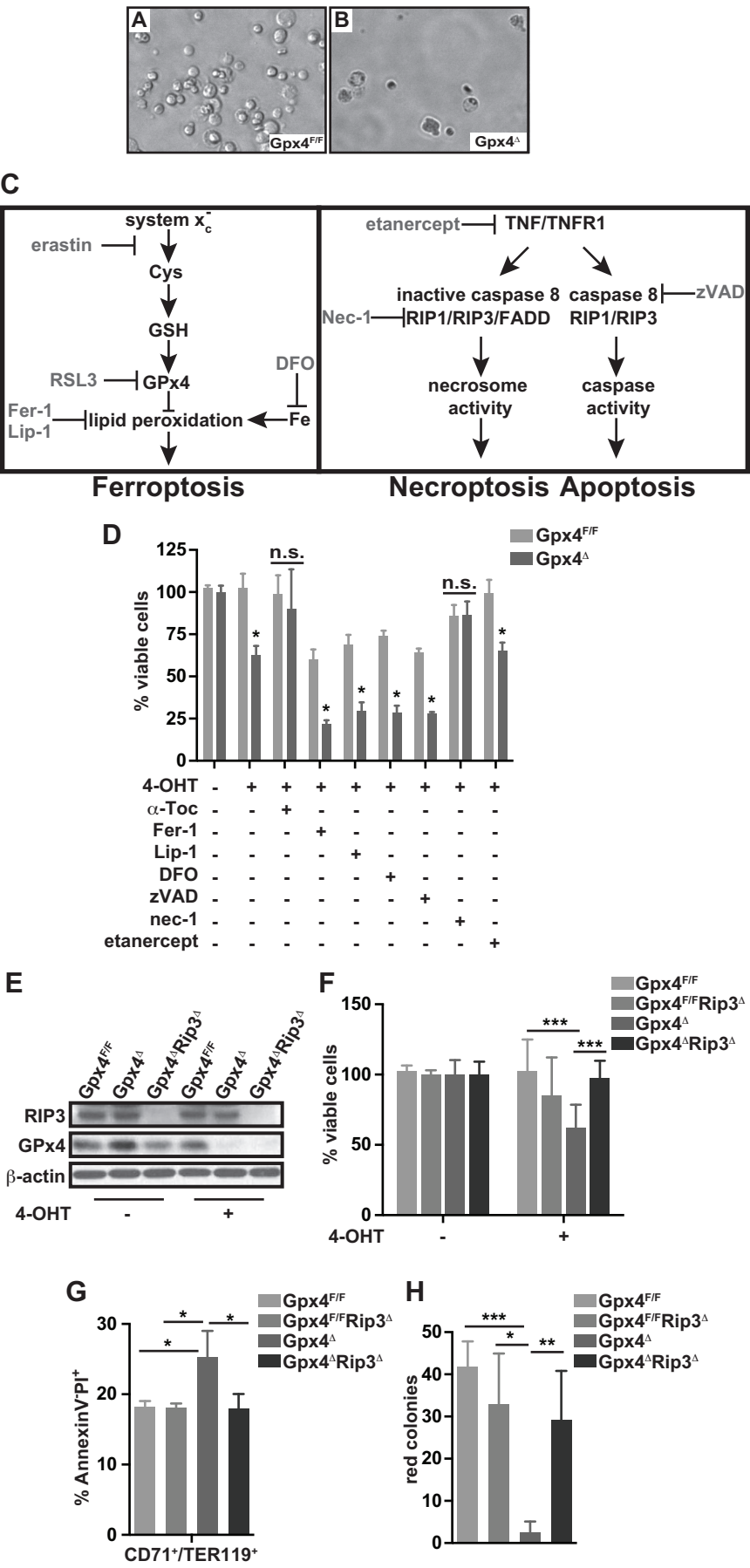
A
Gpx4F/F
B
Gpx4Δ
C
system xc-
erastin
Cys
GSH
RSL3
GPx4
DFO
Fer-1
Lip-1
lipid peroxidation
Fe
etanercept
TNF/TNFR1
inactive caspase 8
caspase 8
zVAD
Nec-1
RIP1/RIP3/FADD
RIP1/RIP3
necrosome activity
caspase activity
Ferroptosis
Necroptosis Apoptosis
D
Gpx4F/F
Gpx4Δ
% viable cells
n.s.
4-OHT
α-Toc
Fer-1
Lip-1
DFO
zVAD
nec-1
etanercept
E
Gpx4F/F
Gpx4Δ
Gpx4ΔRip3Δ
RIP3
GPx4
β-actin
4-OHT
F
Gpx4F/F
Gpx4F/FRip3Δ
Gpx4Δ
Gpx4ΔRip3Δ
% viable cells
4-OHT
G
% AnnexinV-PI+
CD71+/TER119+
H
red colonies

Figure 5

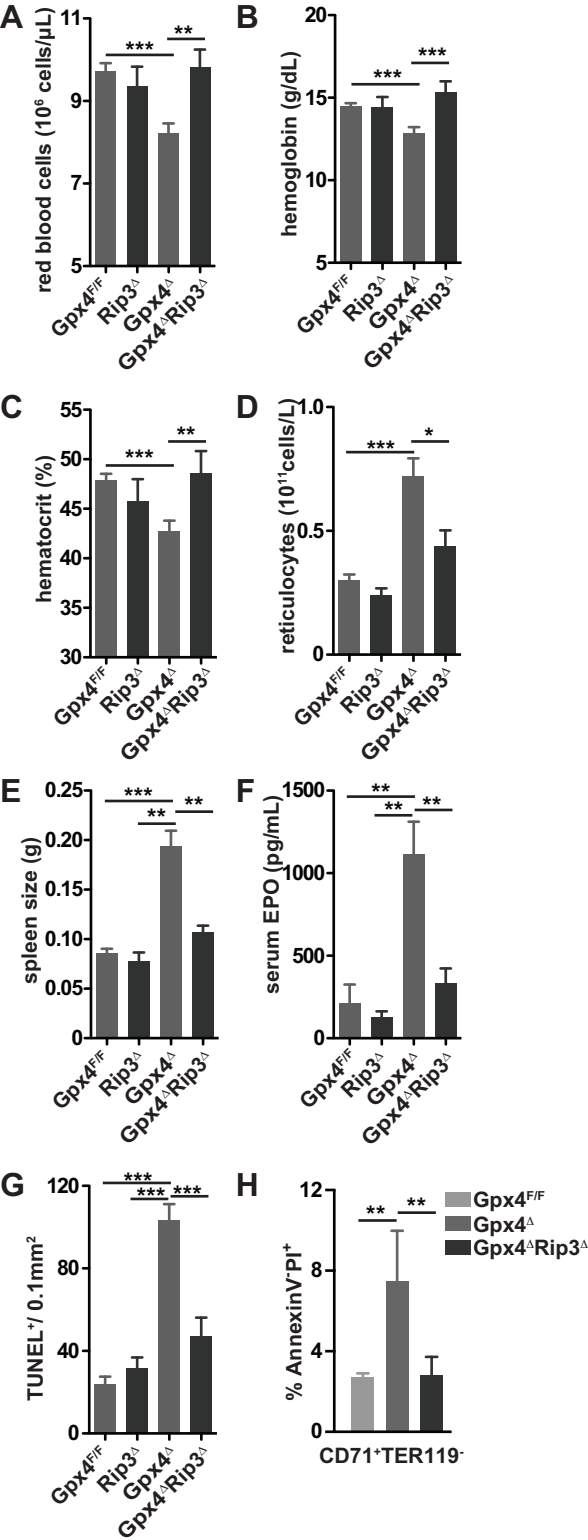
A
red blood cells (10^6 cells/μL)
11
9
7
5
***
**
Gpx4^F/F
Rip3^Δ
Gpx4^Δ
Gpx4^ΔRip3^Δ
B
hemoglobin (g/dL)
20
15
10
5
***
***
C
hematocrit (%)
55
50
45
40
35
30
***
**
D
reticulocytes (10^11 cells/L)
1.0
0.5
0
***
*
E
spleen size (g)
0.25
0.20
0.15
0.10
0.05
0
***
**
**
F
serum EPO (pg/mL)
1500
1000
500
0
**
**
**
G
TUNEL+/ 0.1mm2
120
80
40
0
***
***
***
H
% AnnexinV-PI+
12
8
4
0
**
**
CD71+TER119-
Gpx4^F/F
Gpx4^Δ
Gpx4^ΔRip3^Δ

Figure 6

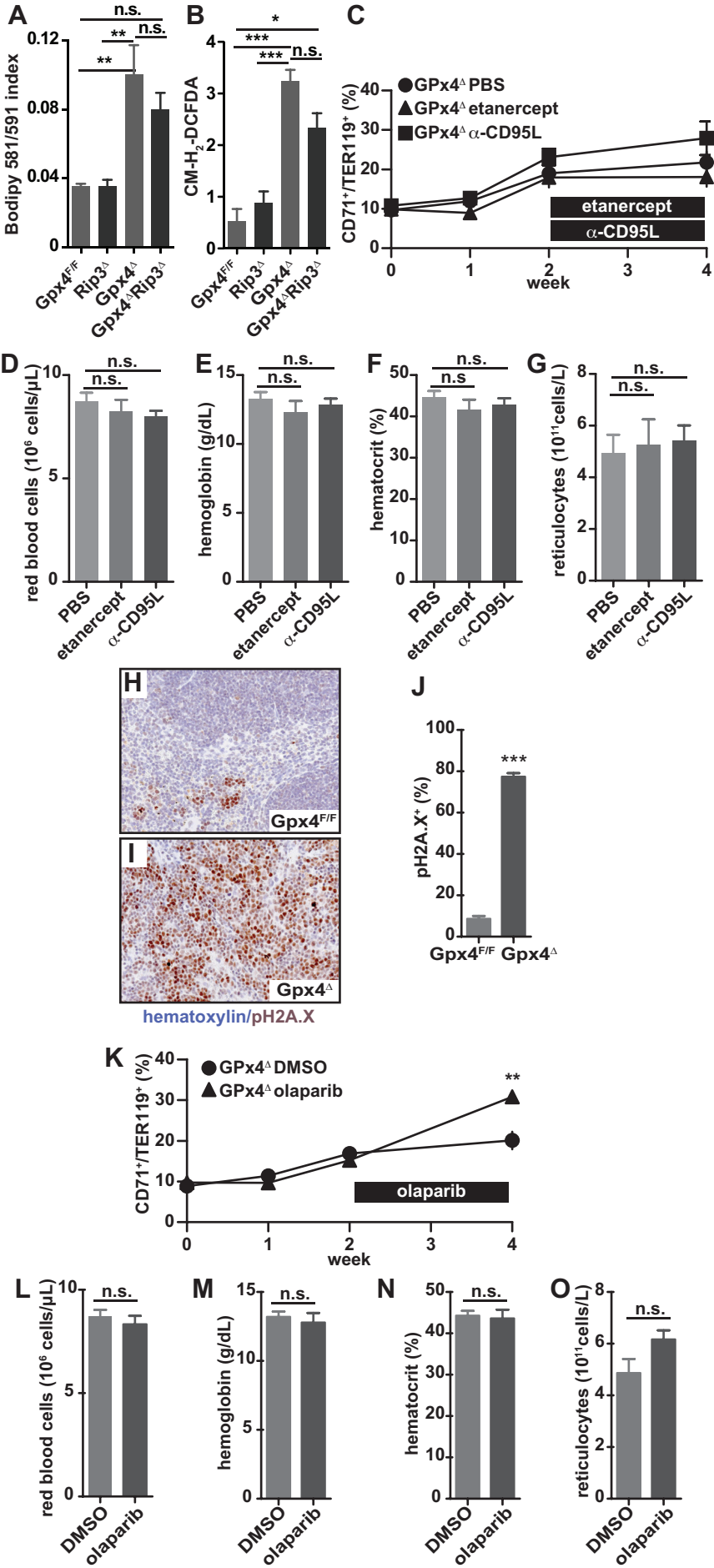
A
Bodipy 581/591 index
0.12
0.08
0.04
0
n.s.
**
n.s.
**
Gpx4F/F
Rip3Δ
Gpx4Δ
Gpx4ΔRip3Δ
B
CM-H2-DCFDA
4
3
2
1
0
*
***
***
n.s.
Gpx4F/F
Rip3Δ
Gpx4Δ
Gpx4ΔRip3Δ
C
CD71+/TER119+ (%)
40
30
20
10
0
GPx4Δ PBS
GPx4Δ etanercept
GPx4Δ α-CD95L
etanercept
α-CD95L
0
1
2
3
4
week
D
red blood cells (10^6 cells/μL)
10
5
0
n.s.
n.s.
PBS
etanercept
α-CD95L
E
hemoglobin (g/dL)
15
10
5
0
n.s.
n.s.
PBS
etanercept
α-CD95L
F
hematocrit (%)
50
40
30
20
10
0
n.s.
n.s
PBS
etanercept
α-CD95L
G
reticulocytes (10^11 cells/L)
8
6
4
2
0
n.s.
n.s.
PBS
etanercept
α-CD95L
H
Gpx4F/F
I
Gpx4Δ
hematoxylin/pH2A.X
J
pH2A.X+ (%)
100
80
60
40
20
0
***
Gpx4F/F
Gpx4Δ
K
CD71+/TER119+ (%)
40
30
20
10
0
GPx4Δ DMSO
GPx4Δ olaparib
**
olaparib
0
1
2
3
4
week
L
red blood cells (10^6 cells/μL)
10
5
0
n.s.
DMSO
olaparib
M
hemoglobin (g/dL)
15
10
5
0
n.s.
DMSO
olaparib
N
hematocrit (%)
50
40
30
20
10
0
n.s.
DMSO
olaparib
O
reticulocytes (10^11 cells/L)
8
6
4
2
0
n.s.
DMSO
olaparib

Figure 7

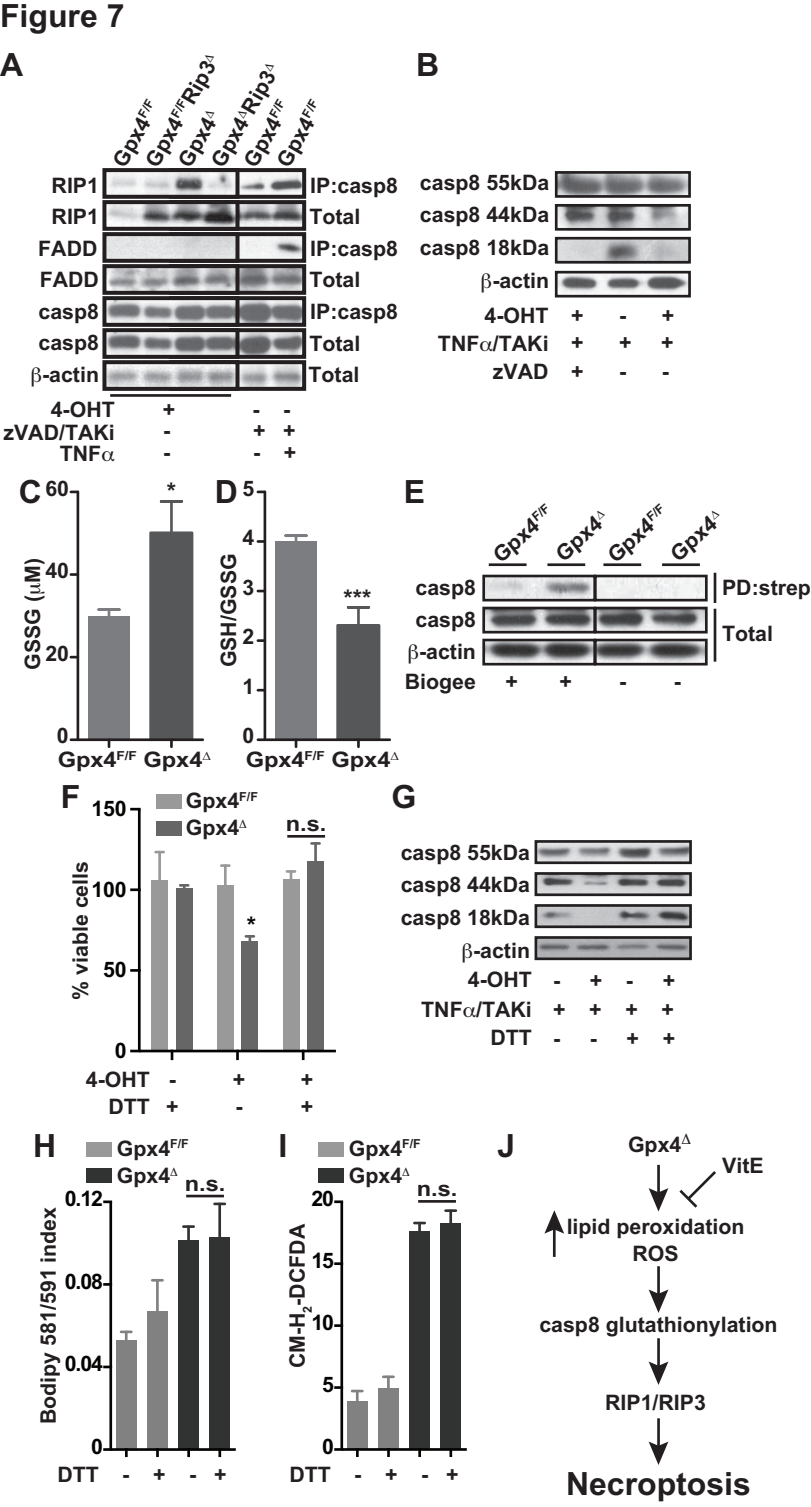
A
Gpx4F/F
Gpx4F/FRip3Δ
Gpx4Δ
Gpx4ΔRip3Δ
Gpx4F/F
Gpx4F/F
RIP1
RIP1
FADD
FADD
casp8
casp8
β-actin
IP:casp8
Total
IP:casp8
Total
IP:casp8
Total
Total
4-OHT + - -
zVAD/TAKi - + +
TNFα - - +
B
casp8 55kDa
casp8 44kDa
casp8 18kDa
β-actin
4-OHT + - +
TNFα/TAKi + + +
zVAD + - -
C
GSSG (μM)
60
40
20
0
*
Gpx4F/F
Gpx4Δ
D
GSH/GSSG
5
4
3
2
1
0
***
Gpx4F/F
Gpx4Δ
E
Gpx4F/F
Gpx4Δ
Gpx4F/F
Gpx4Δ
casp8
casp8
β-actin
PD:strep
Total
Biogee + + - -
F
Gpx4F/F
Gpx4Δ
% viable cells
150
100
50
0
*
n.s.
4-OHT - + +
DTT + - +
G
casp8 55kDa
casp8 44kDa
casp8 18kDa
β-actin
4-OHT - + - +
TNFα/TAKi + + + +
DTT - - + +
H
Gpx4F/F
Gpx4Δ
Bodipy 581/591 index
0.12
0.08
0.04
0
n.s.
DTT - + - +
I
Gpx4F/F
Gpx4Δ
CM-H2-DCFDA
20
15
10
5
0
n.s.
DTT - + - +
J
Gpx4Δ
VitE
lipid peroxidation
ROS
casp8 glutathionylation
RIP1/RIP3
Necroptosis

blood

Prepublished online October 13, 2015;
doi:10.1182/blood-2015-06-654194

Glutathione peroxidase 4 prevents necroptosis in mouse erythroid precursors

Özge Canli, Yasemin B. Alankus, Sasker Grootjans, Naidu Vegi, Lothar Hültner, Philipp S. Hoppe, Timm Schroeder, Peter Vandenabeele, Georg W. Bornkamm and Florian R. Greten

Blood (print ISSN 0006-4971, online ISSN 1528-0020), is published weekly by the American Society of Hematology, 2021 L St, NW, Suite 900, Washington DC 20036.